metals

MDPI

Article

Metal Transfer Behavior of Metal-Cored Arc Welding in Pure Argon Shielding Gas

Ngoc Quang Trinh [1,2], Shinichi Tashiro [1,*], Tetsuo Suga [1], Tomonori Kakizaki [3], Kei Yamazaki [3], Ackadech Lersvanichkool [4], Hanh Van Bui [2] and Manabu Tanaka [1]

[1] Joining and Welding Research Institute, Osaka University, Osaka 567-0047, Japan
[2] School of Mechanical Engineering, Hanoi University of Science and Technology, Hanoi 100-000, Vietnam
[3] Kobe Steel, Ltd., Fujisawa 251-8551, Japan
[4] Thai Kobelco Welding Co., Ltd., Muang 10280, Thailand
* Correspondence: tashiro@jwri.osaka-u.ac.jp; Tel.: +81-6-6879-8666

Abstract: The metal transfer behavior of gas metal arc welding in a pure argon shielding gas was evaluated through experiments using a standard solid wire and a metal-cored wire. The investigation was conducted using observation techniques based on recording images by a high-speed camera equipped with laser assistance and bandpass filters in a range of welding currents. It was observed that the metal transfer mode became a streaming transfer mode when the welding current increased in the solid wire. Meanwhile, in the metal-cored wire, the droplet transfer frequency increased, and the droplet diameter decreased without changing the metal transfer mode in the globular transfer mode. We surmised that the streaming transfer in the solid wire would be caused by the spread of argon plasma at the wire tip, which decreases the effect of the electromagnetic force on droplet detachment. Conversely, due to the presence of flux inside the metal-cored wire, the argon plasma could not spread and was attached close to the iron vapor plasma at the overhead of the droplet. Hence, the electromagnetic force acting on the side of the unmelted flux was ineffective at promoting droplet detachment, preventing the transition to a streaming transfer mode. Furthermore, weld bead formation in the metal-cored wire was better than that in a conventional solid wire.

Keywords: metal-cored arc welding; metal-cored wire; pure argon; shielding gas; droplet transfer; current path

Citation: Trinh, N.Q.; Tashiro, S.; Suga, T.; Kakizaki, T.; Yamazaki, K.; Lersvanichkool, A.; Bui, H.V.; Tanaka, M. Metal Transfer Behavior of Metal-Cored Arc Welding in Pure Argon Shielding Gas. *Metals* **2022**, *12*, 1577. https://doi.org/10.3390/met12101577

Academic Editor: Xiangdong Gao

Received: 31 August 2022
Accepted: 19 September 2022
Published: 23 September 2022

1. Introduction

Gas metal arc welding (GMAW) is a common welding process in the automotive and structural construction industries. During the process, a consumable electrode is melted, and the transfer process of molten metal strongly affects arc stability and welding performance [1,2]. To achieve a weld with the desired quality, various welding parameters must be controlled, among which the welding current and shielding gas are two dominant factors in the metal transfer process [3,4].

When a conventional solid wire electrode is used in GMAW, the metal transfer mode can be classified as a short-circuit, globular, or spray transfer mode [5,6]. The transition between these transfer modes is dependent on the shielding gas components and welding current. It was reported that in a pure CO_2 shielding gas, only a globular transfer mode was observed [7]. On the other hand, when a pure argon shielding gas is used, the metal transfer mode changes from a short-circuit mode to a globular transfer mode and then becomes a spray transfer mode with a gradually increasing welding current [8]. The welding current range between these transfer modes is called the transition current, and its value will increase with an increase in the CO_2 ratio in a pure argon shielding gas when a mixture of the two gases is used [9]. The mechanism of change to the transfer mode depends on the balance of the driving forces acting on the molten droplet at the tip of the wire, in which

the main forces supporting the metal droplet detachment are the electromagnetic force, gravity, and gas drag force, while the resisting forces include the surface tension force and arc pressure [10].

When flux-cored arc welding (FCAW) is carried out by using a tubular wire consisting of a metal sheath filled with inner flux powder, the metal transfer becomes more complex because of the complication of the wire structure and composition. For example, Wang et al. [11] measured the electrical arc signals and droplet transfer of a flux-cored wire in an Ar + 20% CO_2 shielding gas. They reported that both the variation in welding voltage and Fourier transform spectral could determine the metal transfer mode, where two or more transfer modes coexisted at the same time. Bauné et al. [12] assessed the metal transfer behavior in FCAW. They observed that a high droplet transfer frequency with a narrow droplet size distribution would result in a minimized spatter generation. The composition of the flux can strongly affect the metal transfer. Trinh et al. [13] observed that when sodium was added to the flux, the transfer frequency significantly increased. Due to the low boiling point and low ionization of sodium, the presence of sodium plasma facilitated a new current path directly from the neck of molten metal to the weld pool to bypass the inside of the droplet. Therefore, the current of the iron plasma flowing from the bottom of the droplet was limited, thereby reducing the arc pressure, and the electromagnetic force acting on the neck of the droplet was enhanced, thereby promoting droplet detachment. This result was consistent with the study of Valensi et al. [14] regarding the effect of alkaline elements on the stability of a spray arc. The presence of fluoride in the flux was reported to result in a reduction in the hydrogen content of a weld [15,16]. In addition, wire structures, such as metal sheath geometry and flux ratio, also play an important role in the transfer stability and fume formation rate [17–19].

The literature described above indicates that the metal transfer behavior in GMAW can be influenced by various parameters. The influence of a shielding gas on the welding process with solid wire has been studied extensively through both experimental and simulation approaches [20,21]. However, there has been little research conducted on flux-cored wire, especially a metal-type flux-cored wire, whose flux composition consists mostly of iron powder and a small number of alloys. Starling and Modenesi [22] studied the effect of flux composition on welding ability. Their report indicates that the metal transfer behavior of a metal-cored wire is similar to that of a solid wire when using a shielding gas of argon +25% CO_2 and pure CO_2. Suzuki [23] reported briefly on the solutions developed by Kobe Steel (Fujisawa, Japan) for welding quality control and arc stability through a combination of welding wire electrodes and shielding gases. It was qualitatively mentioned that the metal-cored wire can stabilize the welding arc when used with a pure argon shielding gas. However, the mechanism underlying that phenomenon has not been elucidated.

In this study, for the first time, we quantitatively evaluate the metal transfer behavior of metal-cored wire in a pure argon shielding gas, including the metal transfer frequency and droplet diameter, as well as the metal transfer mode, and then compare it with solid wire. The experiment is carried out in a welding current range from 220 A to 280 A, including three welding current levels. Through some setups using high-speed camera observations, the difference in metal transfer behavior between the two wires is clarified.

2. Experimental Procedure

2.1. Common Welding Conditions

In this study, bead-on-plate welding is carried out using a mild steel plate (SS400—JIS G 3101), with the dimensions of 300 mm × 50 mm × 9 mm, as a base metal. We compare the metal transfer behavior of a solid wire and a metal flux-cored wire with the same diameter of 1.2 mm, in which the solid wire is a commercial solid wire (JIS Z3312 YGW11) with an AWS classification that corresponds to A5.18 ER70S-G, and the metal flux-cored wire corresponds to an AWS classification of A5.20 E70T-1C. A list of the chemical compositions of the two wires is shown in Table 1.

Table 1. Chemical composition (mass%) of investigated wires.

Wire	C	Si	Mn	Cu	Al	Ti + Zr	SiO_2	TiO_2
Solid wire	0.04	0.73	1.58	0.23	-	0.22	-	-
Metal-cored wire	0.04	0.90	2.00	-	0.26	-	0.23	0.33

The experimental welding process was conducted using a welding power source (DP-350 OTC Daihen, Kobe, Japan) in direct current electrode positive (DCEP) mode. Two wires were investigated under the three levels of welding current at 220 A, 250 A and 280 A, which correspond to low current, medium current, and high current, respectively. A pure argon gas with a flow rate of 20 L/min was used as the shielding gas. We adjusted the welding voltage from 23.0 V to 29.5 V to maintain a constant arc length of around 6 mm. A contact tip-to-work distance of 20 mm was applied during the process. The base metal plates were moved at 5 mm/s using an actuator. A summary of the welding conditions is presented in Table 2.

Table 2. Welding conditions.

Number	Wire	Current Level (A)	Wire Feed Speed (m/min)	Setting Voltage (V)
01	Solid wire	220	6.9	26
02		250	8.2	28
03		280	8.9	30
04	Metal-cored wire	220	7.3	24
05		250	8.9	25.5
06		280	10.2	27

2.2. Observation Conditions

A photo of the actual experimental setup and a schematic illustrating the experimental setup are shown in Figure 1. A shadowgraph technique was applied using a system consisting of a laser-optical apparatus and a high-speed camera [24]. To clearly visualize the droplet transfer mode, the high-speed camera (Memrecam Q1v, Nac Image Technology, Minato, Japan) was used with five neutral-density filters (ND8) to reduce strong radiation from the arc plasma. An optical lens (AF Micro-NIKKOR, Nikon, Minato, Japan) with a focal length of 105 mm and a focal ratio of 1/2.8 was used. The aperture value was set to f/5.6. The wire tip and molten droplet were illuminated from the back side of the welding torch by using a laser light with a wavelength of 640 nm produced from a lase unit (Calilux HF system, Cavitar, Tampere, Finland), which allows the camera to obtain the shadowgraph images of the objects. The visualization was carried out at a frame rate of 4000 fps, with an exposure time of 20 μs.

It was reported that in the solid wire arc welding process with a pure argon shielding gas, the arc had double layers containing an iron plasma in the center covered by an argon plasma layer [25]. We expected that a similar phenomenon could be observed in metal-cored arc welding. For this purpose, we set up a spectral analysis experiment similar to the experiment of Trinh et al. [13]. Here, two types of filters were employed. The first filter had a nominal central wavelength of 540.0 nm and a full width at half maximum (FWHM) of 10.0 nm (termed the "Fe I filter") to observe the Fe I line spectrum. The second filter had a central wavelength of 696.5 nm and an FWHM of 10 nm to observe the Ar I line spectrum (termed the "Ar I filter"). In this setup, the frame rate of the high-speed camera was 8000 fps, and the exposure time was 20 μs. From that, we could clarify the spatial structure of the arc plasma with a solid wire and metal-cored wire.

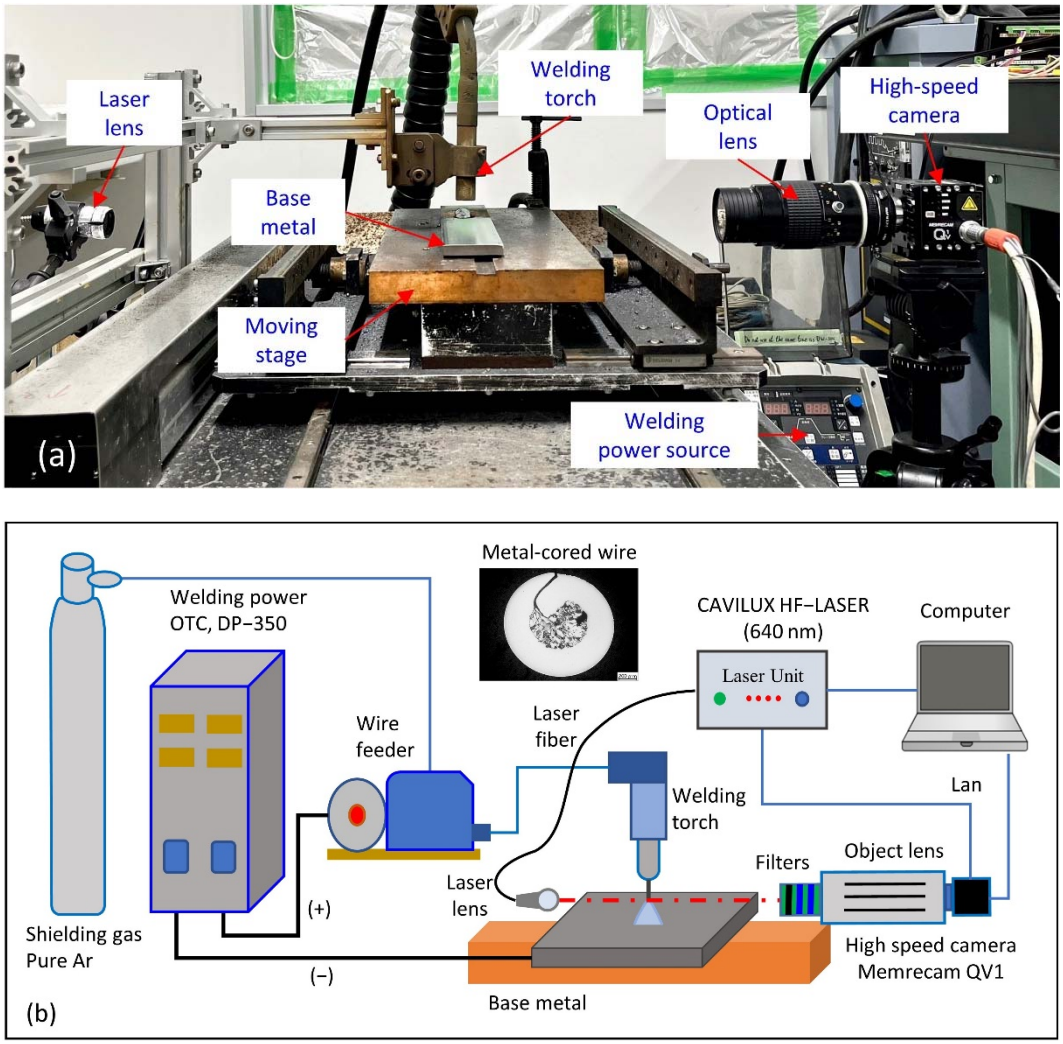

Figure 1. Photo of the experimental setup (**a**) and schematic illustration of experimental apparatus (**b**).

3. Results and Discussion

3.1. Metal Transfer Behavior

Figure 2 shows the metal transfer behavior of the solid wire in three levels of welding current. Using the shadowgraph technique, the morphology of the molten metal droplets was obviously observed under strong radiation emission from the arc. In Figure 2a, an evolution of the arc and droplet at 220 A is depicted in one cycle. At 0 ms, a metal droplet detached from the electrode. The droplet was transferred inside the arc to the weld pool, as shown from 0.75 ms to 3.5 ms. At 0.75 ms, the arc moved from the bottom of the droplet to the wire tip. Another droplet formed and gradually grew from 1.5 ms to 5.75 ms. It completely detached at 6.5 ms. In this case, the arc covered a part of the droplet and concentrated at the bottom of the droplet. In a pure Ar shielding gas, it was reported that the transition current was around 220 A. It can be observed in Figure 2a that the droplet diameter is almost equal to the wire diameter. When the welding current increased to 250 A, the metal transfer mode changed to streaming transfer mode, as shown in Figure 2b. In this case, a long-tapered part was observed at the tip of the wire. The molten metal transferred to the weld pool as a long liquid column, as shown at 0 ms. From 0.25 ms to 3 ms, the arc was always attached to the wire tip while the molten metal was generated and transferred below the attachment point. In the last frame at 3.25 ms, the column of liquid metal totally detached from the tip of the tapered metal. The streaming transfer mode was continually observed at 280 A in Figure 2c. The metal transfer behavior was similar to that found at

250 A in Figure 2b. In this condition, the cycle time for a liquid column metal transfer to the base metal slightly decreased to 2.75 ms.

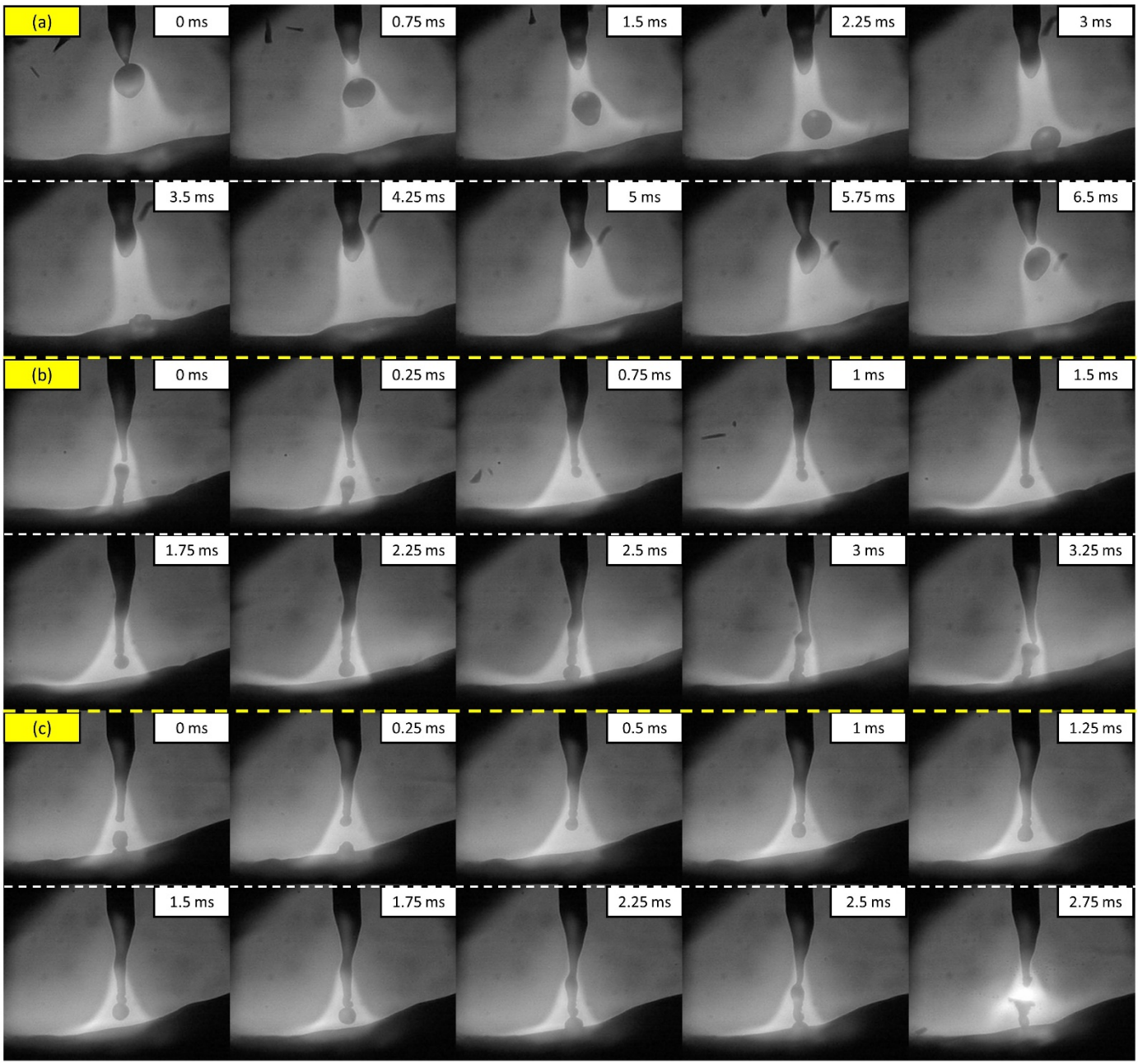

Figure 2. Sequential images of metal transfer in solid wire in 220 A (**a**), 250 A (**b**), and 280 A (**c**) of welding current.

Figure 3 depicts the droplet transfer behavior of the metal-cored wire in the three levels of welding current. Figure 3a presents a transfer cycle at 220 A, where a droplet detached from the wire at 0 ms. Another droplet was subsequently generated at 5.75 ms. Its size gradually increased from 8.5 ms to 22.75 ms, and the detachment occurred at 25.5 ms. Figure 3b shows the transfer in the medium-current range. After the detachment of the initial droplet at 0 ms, the next droplet expanded from 3 ms to 12 ms, and the transfer was completed after 13.5 ms. Figure 3c presents that increasing the welding current to 280 A reduced the period of metal transfer to 9.75 ms. Hence, increasing the welding current from 220 A to 250 A, and 280 A decreased the time for a droplet to transfer from the wire tip to the weld pool from 25.5 ms to 13.5 ms, and 9.75 ms, respectively. Here, during the

transfer period, almost no taper part was observed in the metal-cored wire. With all levels of welding current, the droplet diameter in the metal-cored wire was observed to be larger than the wire diameter.

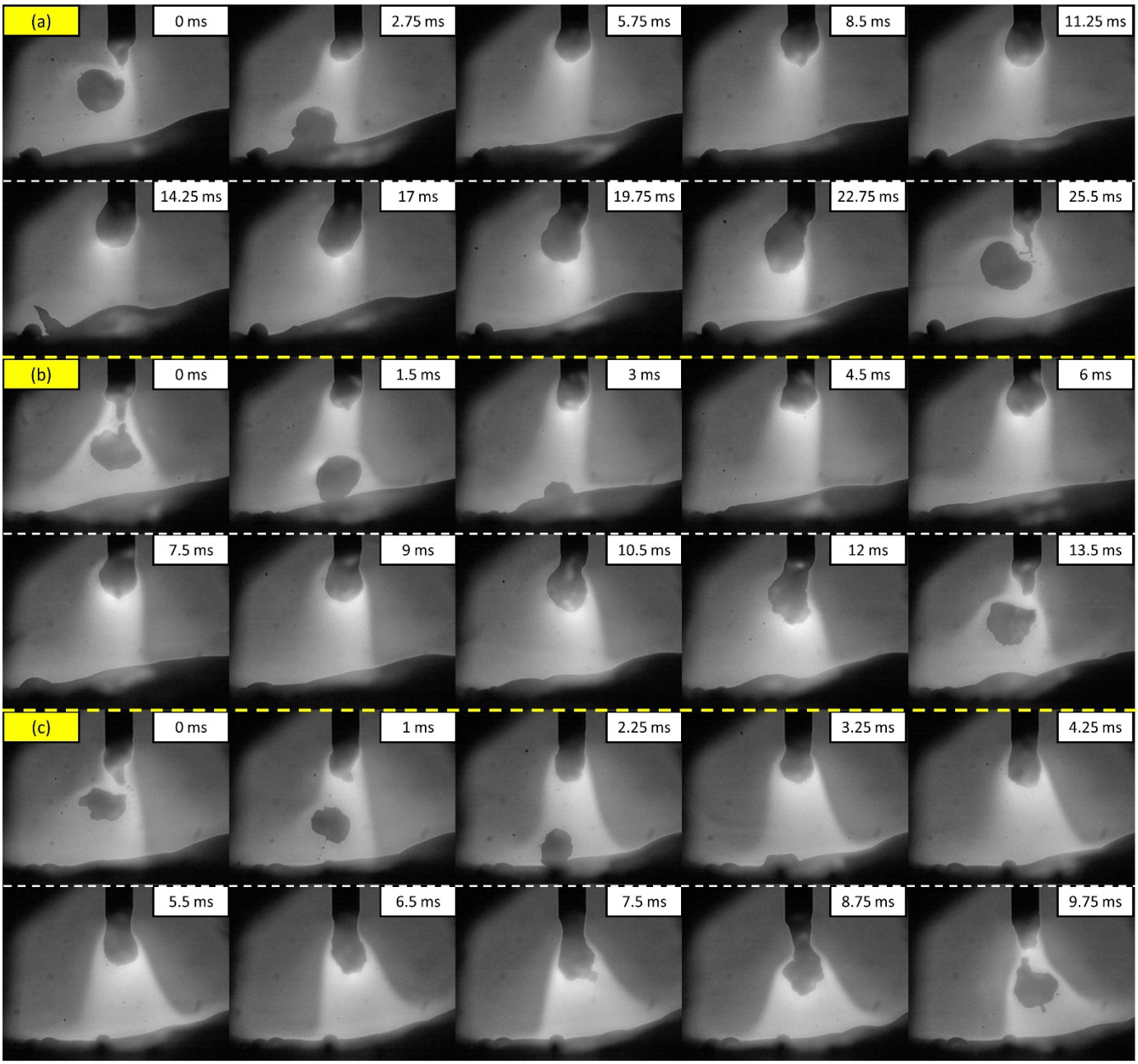

Figure 3. Sequential images of metal transfer in metal-cored wire in 220 A (**a**), 250 A (**b**), and 280 A (**c**) of welding current.

Figure 4 shows the droplet transfer frequencies and the calculated droplet diameters of metal-cored wire in all welding currents. The transfer frequency data are calculated from five measurements, while the error bars indicate the standard deviation. Due to the change in the metal transfer mode at 250 A in the solid wire, the droplet transfer frequency of that wire was not reported. In this figure, the primary axis indicates the droplet transfer frequency, while the secondary axis indicates the droplet diameter. A green line at 1.2 mm presents the wire diameters. It was observed that the droplet transfer frequency increased when the welding current increased. This frequency was promoted from 42.58 Hz to 73.86 Hz, and 119.09 Hz for 220 A, 250 A, and 280 A, respectively.

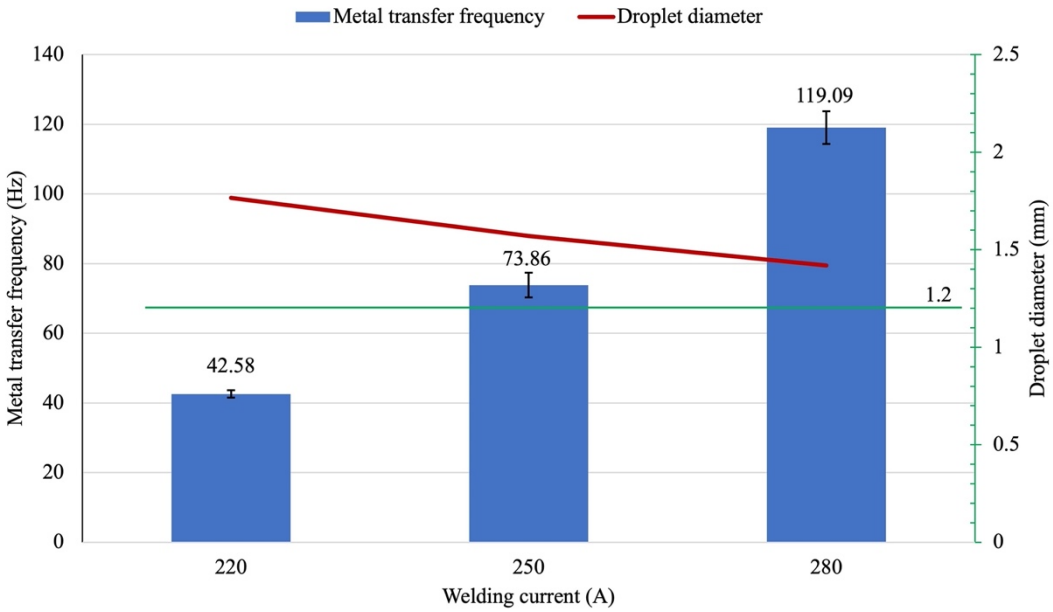

Figure 4. Metal transfer frequency and droplet diameter of metal-cored wire.

In this study, we assume that the melting velocity of the wire is equal to the wire feed speed, and the mass density of a droplet is equal to pure iron. The volume of a droplet can be calculated as follows:

$$V = \frac{D_w \times v_{wfs}}{f \times \rho_{Fe}}$$

where V is the droplet volume (m^3), D_w is the weight of the wire in a unit length (kg/m), v_{wfs} is the wire feed speed (m/s), f is the metal transfer frequency (Hz), and ρ_{Fe} is the mass density of pure iron (kg/m^3).

We assume the droplet was spherical during the transfer process to the weld pool. The droplet diameter was calculated from the droplet volume based on the equation:

$$D = \sqrt[3]{\frac{6 \times V}{\pi}}$$

where D is the droplet diameter (m).

It was observed that the droplet diameter decreased when the welding current increased. However, the calculated droplet diameters were higher than the wire diameter, which indicates that the metal transfer mode of the metal-cored wire was a globular transfer mode in these welding conditions. For the first time, the metal transfer frequency of a metal-cored wire was quantitatively reported in pure Ar at welding currents of 220 A, 250 A, and 280 A. In the welding process with a pure Ar shielding gas, the arc pressure under the droplet was thought to be low, causing the droplet to transfer smoothly through the center of the arc to the weld pool as presented in Figure 3.

3.2. Spectroscopic Observation

In this study, we investigated the distributions of iron plasma and argon plasma in the entire arc plasma at the high current range. Figure 5 presents the observation results of the solid wire in the streaming transfer mode. The sequential images are shown in the period of 2.625 ms, including a one-cycle transfer of molten metal. In Figure 5a, the distribution of iron plasma was obtained using an Fe I filter. The iron vapor concentrated around the transferred liquid column from the wire tip to the surface of the base metal. The iron vapor was generated at the tip of the wire, which had a higher position than the detachment points of molten metal. The argon plasma obtained by Ar I filter is presented in Figure 5b. The argon plasma was observed to distribute in a larger area than the iron

plasma. The outer-argon plasma was clearly separated and covered the inner-iron plasma, which established a dual structure of arc plasma in the solid wire.

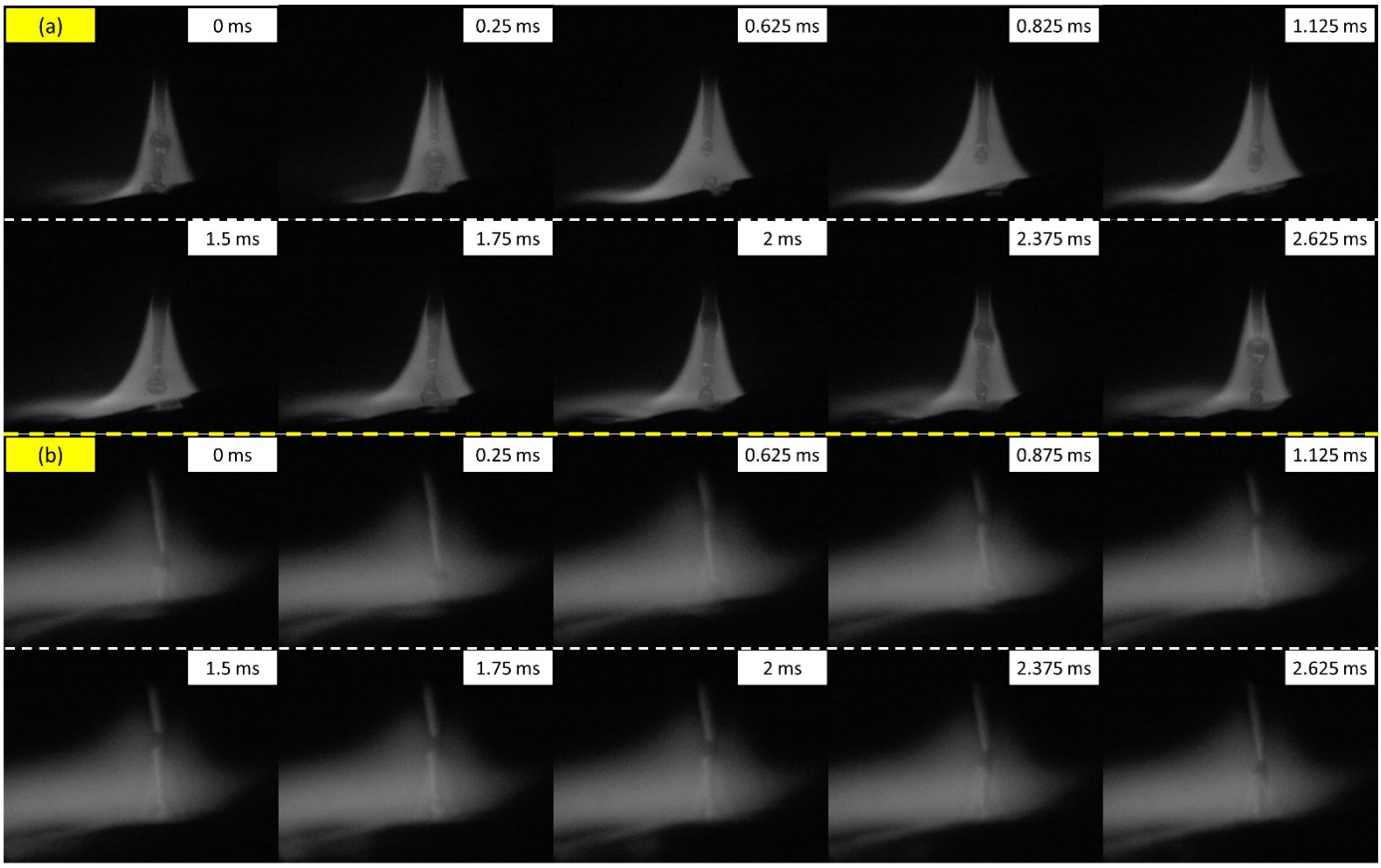

Figure 5. Sequential video images observed with Fe I filter (**a**) and Ar I filter (**b**) of solid wire at 280 A welding current.

Figure 6 shows the droplet transfer observation of the metal-cored wire at 280 A of welding current, using an Fe I filter in Figure 6a and an Ar I filter in Figure 6b. In Figure 6a, it can be observed that the iron plasma attached under the bottom of the droplet as shown at 1 ms. During the expansion of the molten droplets, the iron plasma covered a large area of the droplet before the droplet detachment at 7.875 ms. In addition, Figure 6b shows the argon plasma distribution, in which the argon plasma and iron plasma were also separated, similar to the solid wire. However, during the expansion of the droplet, the attachment positions of these two plasmas were close to the neck of the droplet, which is obviously different from the solid wire. Two typical images of arc plasma behavior obtained without using any bandpass filter are presented in Figure 7. In Figure 7a, it can be observed that argon plasma attached to the top of the taper liquid metal, while iron plasma attached to the bottom of the taper part at the tip of the solid wire. Meanwhile, in Figure 7b, it can be seen that the argon plasma and iron plasma were closely attached to the liquid metal. In this case, almost no taper was observed at the tip of the metal-cored wire.

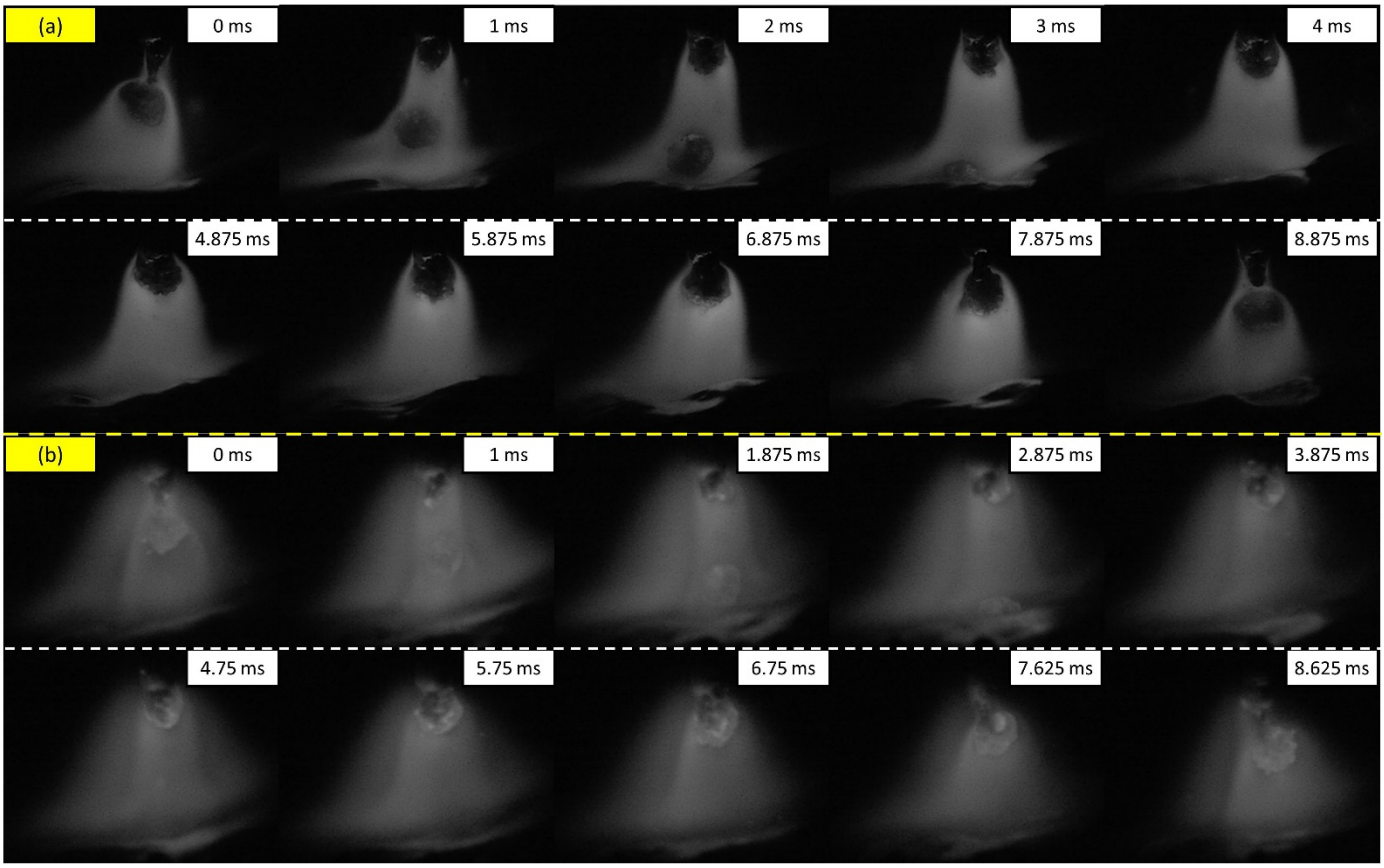

Figure 6. Sequential video images observed with Fe I filter (**a**) and Ar I filter (**b**) of metal-cored wire at 280 A welding current.

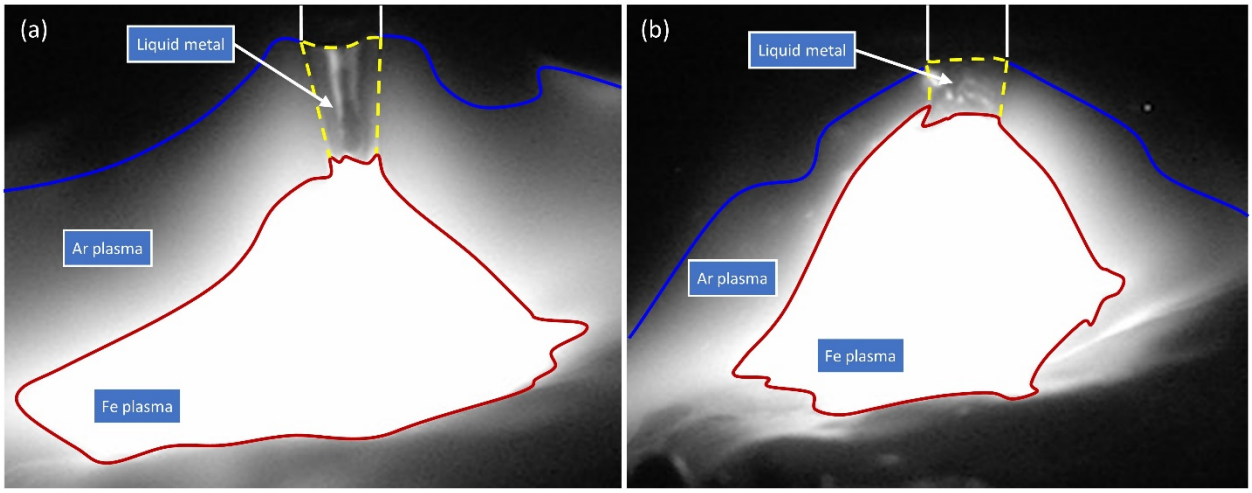

Figure 7. Typical image of arc behavior in solid wire (**a**) and metal-cored wire (**b**) at welding current of 280 A.

A schematic of the metal transfer behavior in two wires at 280 A is depicted in Figure 8 for an explanation of the difference in the metal transfer mode. The current flow inside the solid part of the solid wire was thought to be uniform, as presented in Figure 8a. On the other hand, in the metal-cored wires, due to the low electrical conductivity of the flux, the current flow was concentrated on the outer sheath of the wire, as shown in Figure 8b. Hence, the current density at the interface of the solid part and liquid metal was higher in metal-cored wire than that in the solid wire.

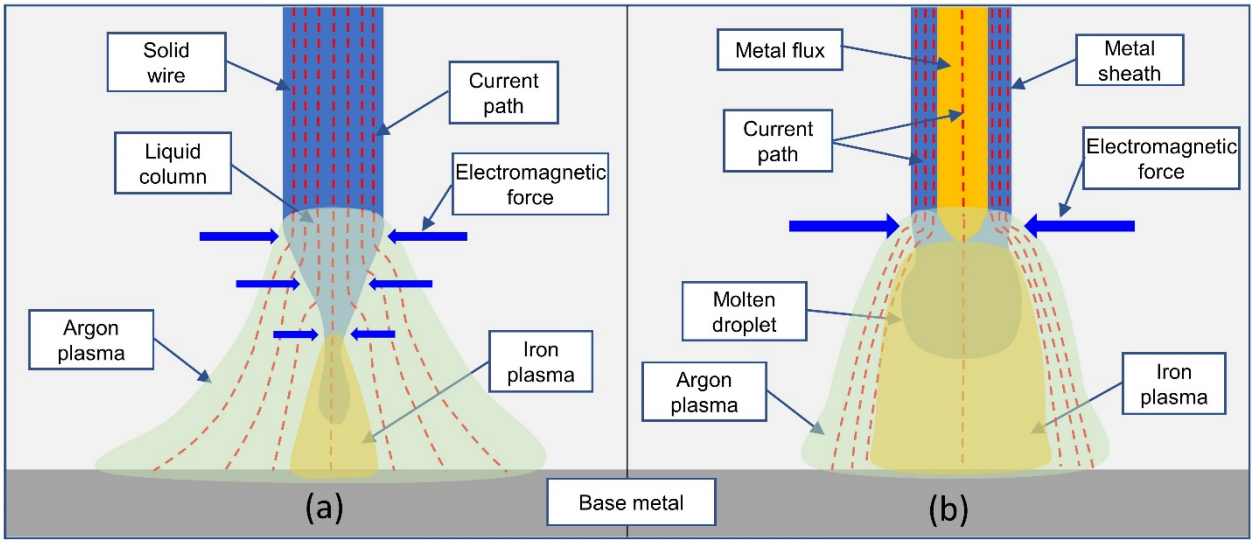

Figure 8. Mechanism of streaming transfer mode in solid wire (**a**) and globular transfer mode in metal-cored wire (**b**).

In Figure 8a, it can be observed that the argon plasma was attached to the side of the wire and spread over a large area. Due to the high electrical conductivity of argon plasma, most of the current was thought to flow through the argon plasma, which leads to the electromagnetic force being spread on the surface of the wire [21,26]. Then, a long-taper liquid column formed at the wire tip. Due to the current flow to the argon plasma through the taper, the amount of current flow through the molten droplet was small, which counteracted the effect of the electromagnetic force on droplet detachment. In Figure 8b, it can be seen that the argon plasma and iron plasma were closely attached at the overhead of the droplet. In this case, the presence of a flux column limited the current flow inward from the wire sheath to the molten droplet, which prevented the liquid column formation. This implies that the radiation loss in metal-cored wire can occur up to a higher position than that in the solid wire, which results in the current mostly flowing through the molten metal on the side of the unmelted flux to the argon plasma. In metal-cored wire, the metal transfer behavior is strongly related to the state of the unmelted flux, as presented in the scanning electron microscopy (SEM) analysis in the investigation of Trinh et al. [18]. In a pure argon shielding gas, the current mostly flows through on the side of the unmelted flux, and the tip of the unmelted flux is thought to reach into the molten droplet, as shown in Figure 8b. Therefore, the electromagnetic force acting on the molten metal on the side of the unmelted flux was ineffective at enhancing droplet detachment, which leads to a globular transfer mode in metal-cored wire. The electromagnetic force directly acting on the neck enhances detachment, but the neck formation is delayed due to the presence of the unmelted flux in this case. The effect of the wire structure on the formation of a liquid column at the wire tip was discussed by Nakamura and Hiraoka [27], in which they investigated the effect of a coaxial multilayer solid wire on the metal transfer behavior in an argon shielding gas. The results indicate that using an inner part that has a lower melting temperature can prevent the streaming transfer mode and improves arc stability. However, we considered that the mechanism in our study is quite different because the electrical conductivity of the flux is low, which limits the melting rate of the flux by Joule heating when compared to a coaxial solid wire.

In the GMAW process, the metal transfer mode has an important role in determining welding quality and the stability of the process. When the free-flight transfer mode was utilized, the spray transfer mode was the most desirable due to the low workability of the globular transfer mode. The projected spray transfer mode has a higher metal transfer frequency, which leads to a lower spatter and fume formation rate than that of the globular transfer mode [28]. However, when the current exceeds a critical value, the metal transfer

mode changes from projected transfer mode to streaming transfer mode. With a pure argon shielding gas, the streaming transfer mode is rarely used due to the instability of the arc [29].

During the welding process, the metal transfer process to the weld pool has an intensive influence on the formation and geometry of the weld bead. Over the last decade, real-time monitoring of the welding process has contributed to the control of the width and height of a weld, which has received much attention during GMAW [30] and wire arc additive manufacturing (WAAM) [31]. This study also evaluated weld bead formation after the welding process. Figure 9 shows the weld bead appearances of the solid wire and metal-cored wire at a 280 A welding current. In Figure 9a, due to the unstable liquid column and the instability of the arc, the weld bead of the solid wire began wandering. On the other hand, in Figure 9b, the weld bead is smooth and straight in the metal-cored wire. This result indicates that the metal transfer in a metal-cored wire in a pure argon shielding gas is much more stable than that in a solid wire in the testing condition. Further, the welding performance of metal-cored wire improved by preventing the unstable streaming transfer mode.

Figure 9. Weld bead appearance of solid wire (**a**) and metal-cored wire (**b**) at 280 A welding current.

4. Conclusions

In the current study, we investigated the metal transfer behavior of metal-cored wire in a pure argon shielding gas by using laser assistance and bandpass filter observations. Here, we conducted experiments in a wide range of welding currents and compared a metal-cored wire and solid wire. The conclusions of this study can be drawn as follows:

1 In metal-cored wire, when the welding was increased, the metal- transfer frequency increased, while the droplet diameter decreased.
2 In a pure argon shielding gas, the metal transfer mode of the solid wire changed to a streaming transfer at 250 A of welding current. On the other hand, the metal transfer mode of metal-cored wire was a globular transfer, despite the welding current being high at 280 A.
3 The change in the metal transfer mode in the solid wire was caused by the spread of the argon plasma at the tip of the wire. Meanwhile, in the metal-cored wire, due to the presence of the flux, the argon plasma and iron plasma were closely attached to the overhead of the droplet, where the electromagnetic force, acting on the molten metal on the side of the unmelted flux of the wire, was ineffective at enhancing the metal droplet detachment.

4 The metal-cored wire can limit the instability of the arc during pure argon shielding gas welding, which provides better welding performance compared to conventional solid wire in weld bead formation.

Author Contributions: Conceptualization, methodology, and supervision, S.T.; experiment and writing—original draft preparation, N.Q.T.; writing—review and editing, S.T.; discussion, T.S., T.K., K.Y., A.L., H.V.B., and M.T. All authors have read and agreed to the published version of the manuscript.

Funding: This research received no external funding.

Institutional Review Board Statement: Not applicable.

Informed Consent Statement: Not applicable.

Data Availability Statement: Data can be made available based on the requirements to verify this work.

Acknowledgments: The authors are grateful for the support toward this study provided by a joint research agreement between the Joining and Welding Research Institute, Osaka University, Japan; Hanoi University of Science and Technology, Vietnam; Kobe Steel Ltd., Japan; and Thai Kobelco Welding Co., Ltd., Thailand.

Conflicts of Interest: The authors declare no conflict of interest.

References

1. Lancaster, J.F. The Physics of Fusion Welding Part 2: Mass Transfer and Heat Flow. *IEE Proc. B Electr. Power Appl.* **1987**, *134*, 297–316. [CrossRef]
2. Kah, P.; Latifi, H.; Suoranta, R.; Martikainen, J.; Pirinen, M. Usability of Arc Types in Industrial Welding. *Int. J. Mech. Mater. Eng.* **2014**, *9*, 15. [CrossRef]
3. Rhee, S.; Kannatey-Asibu, E. Observation of Metal Transfer during Gas Metal Arc Welding. *Am. Soc. Mech. Eng. Prod. Eng. Div. PED* **1992**, *51*, 203–213.
4. Nemchinsky, V.A. The Effect of the Type of Plasma Gas on Current Constriction at the Molten Tip of an Arc Electrode. *J. Phys. D Appl. Phys.* **1996**, *29*, 1202–1208. [CrossRef]
5. Izutani, S.; Shimizu, H.; Suzuki, K.; Koshiishi, F. *Observation and Classification of Droplet Transfer in Gas Metal Arc Welding*; IIW Doc. 212-1090-06; International Institute of Welding: Villepinte, France, 2006.
6. Scotti, A.; Ponomarev, V.; Lucas, W. A Scientific Application Oriented Classification for Metal Transfer Modes in GMA Welding. *J. Mater. Process. Technol.* **2012**, *212*, 1406–1413. [CrossRef]
7. Haidar, J.; Lowke, J.J. Effect of CO_2 Shielding Gas on Metal Droplet Formation in Arc Welding. *IEEE Trans. Plasma Sci.* **1997**, *25*, 931–936. [CrossRef]
8. Jönsson, P.G.; Eagar, T.W.; Szekely, J. Heat and Metal Transfer in Gas Metal Arc Welding Using Argon and Helium. *Metall. Mater. Trans. B* **1995**, *26*, 383–395. [CrossRef]
9. Methong, T.; Shigeta, M.; Tanaka, M.; Ikeda, R.; Matsushita, M.; Poopat, B. Visualization of Gas Metal Arc Welding on Globular to Spray Transition Current. *Sci. Technol. Weld. Join.* **2018**, *23*, 87–94. [CrossRef]
10. Hu, J.; Tsai, H.L. Metal Transfer and Arc Plasma in Gas Metal Arc Welding. *J. Heat Transfer.* **2007**, *129*, 1025–1035. [CrossRef]
11. Wang, W.; Liu, S.; Jones, J. Flux Cored Arc Welding: Arc Signals, Processing and Metal Transfer Characterization. *Weld. J. -Incl. Weld. Res. Suppl.* **1995**, *74*, 369s.
12. Bauné, E.; Bonnet, C.; Liu, S. Assessing Metal Transfer Stability and Spatter Severity in Flux Cored Arc Welding. *Sci. Technol. Weld. Join.* **2001**, *6*, 139–148. [CrossRef]
13. Trinh, N.Q.; Tashiro, S.; Tanaka, K.; Suga, T.; Kakizaki, T.; Yamazaki, K.; Morimoto, T.; Shimizu, H.; Lersvanichkool, A.; Murphy, A.B.; et al. Effects of Alkaline Elements on the Metal Transfer Behavior in Metal Cored Arc Welding. *J. Manuf. Process.* **2021**, *68*, 1448–1457. [CrossRef]
14. Valensi, F.; Pellerin, N.; Pellerin, S.; Castillon, Q.; Dzierzega, K.; Briand, F.; Planckaert, J.P. Influence of Wire Initial Composition on Anode Microstructure and on Metal Transfer Mode in GMAW: Noteworthy Role of Alkali Elements. *Plasma Chem. Plasma Process.* **2018**, *38*, 177–205. [CrossRef]
15. Kil, W.; Shin, M.; Bang, K. Effects of Fluoride in the Flux on Hydrogen Content in Weld Metal and Operating Behavior in FCAW-S. *J. Weld. Join.* **2017**, *35*, 65–70. [CrossRef]
16. Bang, K.S.; Jung, H.C.; Han, I.W. Comparison of the Effects of Fluorides in Rutile-Type Flux Cored Wire. *Met. Mater. Int.* **2010**, *16*, 489–494. [CrossRef]

17. Matsuda, F.; Ushio, M.; Tsuji, T.; Mizuta, T. Arc Characteristics and Metal Transfer with Flux-Cored Electrode in CO_2 Shielding (Report I): Effect of Geometrical Shape in Wire Cross-Section on Metal Transfer in Stainless Steel Wire. *Trans. JWRI* **1979**, *8*, 187–192.
18. Trinh, N.Q.; Tashiro, S.; Suga, T.; Kakizaki, T.; Yamazaki, K.; Morimoto, T.; Shimizu, H.; Lersvanichkool, A.; Bui, H.V.; Tanaka, M. Effect of Flux Ratio on Droplet Transfer Behavior in Metal-Cored Arc Welding. *Metals* **2022**, *12*, 1069. [CrossRef]
19. Yamamoto, E.; Yamazaki, K.; Suzuki, K.; Koshiishi, F. Effect of Flux Ratio in Flux-Cored Wire on Wire Melting Behaviour and Fume Emission Rate. *Weld. World* **2010**, *54*, 154–159. [CrossRef]
20. Ushio, M.; Ikeuchi, K.; Tanaka, M.; Seto, T. Effects of Shielding Gas on Metal Transfer. *Weld. Int.* **1995**, *9*, 462–466. [CrossRef]
21. Ogino, Y.; Hirata, Y.; Asai, S. Discussion of the Effect of Shielding Gas and Conductivity of Vapor Core on Metal Transfer Phenomena in Gas Metal Arc Welding by Numerical Simulation. *Plasma Chem. Plasma Process.* **2020**, *40*, 1109–1126. [CrossRef]
22. Starling, C.M.D.; Modenesi, P.J. Metal Transfer Evaluation of Tubular Wires. *Weld. Int.* **2007**, *21*, 412–420. [CrossRef]
23. Suzuki, R. State of the Art of Process Control of Molten Droplet and Pool in Gas Metal Arc Welding. *Weld. Int.* **2012**, *26*, 178–186. [CrossRef]
24. Mamat, S.B.; Tashiro, S.; Tanaka, M.; Yusoff, M. Study on Factors Affecting the Droplet Temperature in Plasma MIG Welding Process. *J. Phys. D Appl. Phys.* **2018**, *51*, 135206. [CrossRef]
25. Rouffet, M.E.; Wendt, M.; Goett, G.; Kozakov, R.; Schoepp, H.; Weltmann, K.D.; Uhrlandt, D. Spectroscopic Investigation of the High-Current Phase of a Pulsed GMAW Process. *J. Phys. D Appl. Phys.* **2010**, *43*, 434003. [CrossRef]
26. Hertel, M.; Trautmann, M.; Jäckel, S.; Füssel, U. The Role of Metal Vapour in Gas Metal Arc Welding and Methods of Combined Experimental and Numerical Process Analysis. *Plasma Chem. Plasma Process.* **2017**, *37*, 531–547. [CrossRef]
27. Nakamura, T.; Hiraoka, K. Effect of Coaxial Welding Wire Structure on Arc Instability in Argon Shielding Gas. *Sci. Technol. Weld. Join.* **2011**, *16*, 717–721. [CrossRef]
28. Bosworth, M.R.; Deam, R.T. Influence of GMAW Droplet Size on Fume Formation Rate. *J. Phys. D Appl. Phys.* **2000**, *33*, 2605–2610. [CrossRef]
29. Modenesi, P.J.; Nixon, J.H. Arc Instability Phenomena in GMA Welding. *AWS Weld. J.* **1994**, *73*, 219–224.
30. Pinto-Lopera, J.E.; Motta, J.M.S.T.; Alfaro, S.C.A. Real-Time Measurement of Width and Height of Weld Beads in GMAW Processes. *Sensors* **2016**, *16*, 1500. [CrossRef] [PubMed]
31. Veiga, F.; Suarez, A.; Aldalur, E.; Artaza, T. Wire Arc Additive Manufacturing of Invar Parts: Bead Geometry and Melt Pool Monitoring. *Meas. J. Int. Meas. Confed.* **2022**, *189*, 110452. [CrossRef]